Calcium-Linked Self-Association of Human Complement C1s̄†

German Rivas,‡ Kenneth C. Ingham,§ and Allen P. Minton*,‡

Laboratory of Biochemical Pharmacology, National Institute of Diabetes and Digestive and Kidney Diseases, National Institutes of Health, Bethesda, Maryland 20892, and Department of Biochemistry, Holland Laboratory, American Red Cross, Rockville, Maryland 20855

Received July 2, 1992; Revised Manuscript Received September 10, 1992

ABSTRACT: The weight-average molecular weight of C1s̄, an activated serine protease subcomponent of human complement C1, has been measured by means of sedimentation equilibrium over a wide range of both protein and calcium ion concentrations. The combined data may be accounted for quantitatively by a simple model for Ca^{2+}-dependent self-association of C1s̄ to a dimer. According to this model, the monomer contains a single Ca^{2+} binding site with $K \cong 3 \times 10^5$ M^{-1}, and the dimer contains three independent Ca binding sites, two having a Ca^{2+} affinity lower than that of the monomer ($K \cong 3 \times 10^4$ M^{-1}). The third binding site in the dimer, which presumably lies at the interface between the two amino-terminal α domains, has a higher Ca^{2+} affinity ($K \cong 1 \times 10^8$ M^{-1}) and provides the driving force for C1s̄ dimerization in the presence of calcium.

The first component of complement, C1, is an enzyme complex composed of three interacting subcomponents, C1q, C1r, and C1s. C1r and C1s are homologous serine protease zymogens that form a Ca^{2+}-dependent heterotetramer, C1s–$(C1r)_2$–C1s, which associates in a 1:1 ratio with C1q to form C1. Upon binding to C1 to several activators, these two zymogens are sequentially activated to C1r̄ and C1s̄, triggering the first step in the activation of complement by the classical pathway (Cooper, 1985; Arlaud et al., 1987a; Schumaker et al., 1987). The mechanism of activation is poorly understood. It seems that activator-induced conformational changes in the recognition component, C1q, subtly affect the interactions between zymogens to facilitate their mutual activation. A more detailed understanding of the activation and regulation of C1 requires better information about the nature of the subcomponent interactions, most of which depend on Ca^{2+}.

C1r self-associates through its C-terminal catalytic region to form a stable dimer in the presence or absence of Ca^{2+}. C1s forms a dimer only in the presence of Ca^{2+} (Valet & Cooper, 1974; Tschopp et al., 1980) and this interaction is mediated through the N-terminal α region of the molecule (Busby & Ingham, 1988, 1990; Thielens et al., 1990a,b). However, in Ca^{2+}-containing mixtures of the two, a heterotetramer C1s–$(C1r)_2$–C1s is formed in which the N-terminal α regions of C1s, instead of binding to themselves, bind to the homologous α regions of C1r (Arlaud et al., 1980, 1986; Tschopp et al., 1980; Villiers et al., 1985; Busby & Ingham, 1990; Thielens et al., 1990a,b; Illy et al., 1991). Equilibrium Ca^{2+} binding isotherms indicate that the heteroassociation (C1r–C1s) involves the binding of two Ca^{2+} ions (one per α region) whereas the homoassociation (C1s–C1s) seems to provide an additional Ca^{2+} binding site (Thielens et al., 1990b; Villiers et al., 1980). Quantitative aspects of the linkage between Ca^{2+} binding and protein–protein interactions have not been explored.

Analytical ultracentrifugation provides a powerful tool for the quantitative characterization of macromolecular associations in solution (Harding & Rowe, 1992; Minton, 1990; Schachman, 1989). Recent technical developments permit the quantitation of absorbance or radioactivity gradients of solute after centrifugation to sedimentation equilibrium in preparative centrifuges [Attri & Minton, 1983, 1986, 1987; reviewed by Howlett (1987), Minton (1989), and Pollet (1985)]. Recently developed tracer methods (Servillo et al., 1981; Attri & Minton, 1986, 1987; Muramatsu & Minton, 1989) provide a means for readily acquiring sedimentation equilibrium data over a range of protein concentrations that is sufficiently broad to permit a proper analysis of reversible protein associations (Muramatsu & Minton, 1989; Hsu & Minton, 1991).

In the present work the weight-average molecular weight (M_w) of human C1s̄ was studied over a broad range of protein and Ca^{2+} concentrations. It was first established that, at each concentration of Ca^{2+}, the dependence of M_w upon protein concentration could be well accounted for by a reversible monomer–dimer equilibrium with an association constant that increased with increasing concentrations of Ca^{2+}. Next, a general model for ligand-linked self-association was constructed and special cases of the model were fitted to the data in order of increasing complexity, to establish the simplest model capable of accounting for the entire set of data in a global fashion. Finally, the Ca^{2+} binding isotherm corresponding to that model was calculated and compared with the results of previously reported binding measurements.

THEORY

Consider a protein existing as an equilibrium mixture of monomer with molecular weight M_1 and dimer with molecular weight $2M_1$:

$$2P \rightleftarrows P_2$$

with equilibrium association constant defined by

$$K = c_2/c_1^2 \quad (1)$$

where c_1 and c_2 are the molar concentrations of monomer and dimer, respectively. The total concentration of protein, in units of moles of monomer per liter, is given by

$$c_{tot} = c_1 + 2c_2 \quad (2)$$

Equations 1 and 2 are solved to yield c_1 and c_2 as functions

† Supported in part by grant HL21791 from the National Institutes of Health

* To whom correspondence should be addressed at Laboratory of Biochemical Pharmacology, NIH, Building 8, Room 226, Bethesda, MD 20892.

‡ NIH.

§ American Red Cross.

0006-2960/92/0431-11707$03.00/0

of K and c_{tot}:

$$c_1 = [-1 + (1 + 8\,Kc_{tot})^{1/2}]/(4K) \quad (3)$$

$$c_2 = Kc_1^2 \quad (4)$$

The weight-average molecular weight is given by

$$M_w = M_1\,(c_1 + 4c_2)/(c_1 + 2c_2) \quad (5)$$

where M_1 is the molecular weight of the C1s polypeptide chain. For simplicity we assume that calcium binds independently to each site in both monomer and dimer. In general there may be more than one class of independent sites on the monomer and dimer. Let $n_{11}, n_{12}, ..., n_{1x}$ represent the number of binding sites in each of x classes on the monomer with respective equilibrium association constants $K_{11}, K_{12}, ..., K_{1x}$. Similarly, let $n_{21}, n_{22}, ..., n_{2y}$ represent the number of sites in each of y classes on the dimer with corresponding association constants $K_{21}, K_{22}, ..., K_{2y}$. The calcium binding isotherms for pure monomer and pure dimer, respectively are given by

$$n_{b1} = \sum_{i=1}^{x} n_{1i}K_{1i}[Ca^{2+}]/(1 + K_{1i}[Ca^{2+}]) \quad (6)$$

and

$$n_{b2} = \sum_{i=1}^{y} n_{2i}K_{2i}[Ca^{2+}]/(1 + K_{2i}[Ca^{2+}]) \quad (7)$$

where n_{b1} and n_{b2} denote the number of moles of calcium bound per mole of monomer and dimer, respectively, and $[Ca^{2+}]$ denotes the molar concentration of free calcium. It follows from linkage theory (Minton, 1975; Record et al., 1978; Saroff, 1991; Wyman & Gill, 1990) that

$$\log K = \log K_0 + \sum_{i=1}^{y} n_{2i} \log (1 + K_{2i}[Ca^{2+}]) - 2\sum_{i=1}^{x} n_{1i} \log (1 + K_{1i}[Ca^{2+}]) \quad (8)$$

where K_0 is the equilibrium constant for protein dimerization in the absence of calcium. The reader may verify that

$$d (\log K)/d (\log [Ca^{2+}]) = n_{b2}([Ca^{2+}]) - 2n_{b1}([Ca^{2+}]) \quad (9)$$

Given the values of K_0, $[Ca^{2+}]$, and c_{tot} and the values of n_{1i}, K_{1i}, n_{2i}, and K_{2i} for all i, the value of M_w is calculated as follows. First K is calculated using eq 8. Next c_1 and c_2 are calculated using eqs 3 and 4. Finally M_w is calculated using eq 5.

The overall binding isotherm is given by

$$n_b([Ca^{2+}]) = \{c_1n_{b1}([Ca^{2+}]) + c_2n_{b2}([Ca^{2+}])\}/c_{tot} \quad (10)$$

where n_b is the number of moles of calcium bound per mole of C1s.

EXPERIMENTAL PROCEDURES

All protein solutions were prepared by dialysis into 25 mM Hepes hydrochloride and 150 mM NaCl, pH 7.4 (Hepes buffer), that had been passed through a chelating filter (Bio-Rex, Bio-Rad) and supplemented with $CaCl_2$ as necessary.

Purification of Human C1s. All experiments were conducted with the activated form of human C1s (C1s), isolated from Cohn fraction I of human plasma by affinity chromatography (Busby & Ingham, 1988). Homogeneity of the protein was checked by SDS–PAGE on a Pharmacia Phastgel system using 8–25% gradient acrylamide gels and by size-exclusion chromatography on Superose 12 (Pharmacia).

^{125}I Labeling of C1s. C1s [250 μL, 0.3–0.5 mg/mL in Hepes buffer [with 5 mM $CaCl_2$ to avoid interference with the dimerization process according to Illy et al. (1991)]] was incubated with one Iodo-Bead (Pierce Chemical Co.) and 0.5 mCi of $Na^{125}I$ (Amersham Corp.) at room temperature for 15 min. The excess free label was removed by extensive dialysis against Hepes buffer. A mixture of labeled and cold C1s was checked by size-exclusion chromatography on a Zorbax G-250 column equilibrated in Hepes buffer with 1 mM EGTA: eluted peaks of absorbance and radioactivity were superimposable. The specific activity ranged from 0.8×10^7 to 1.6×10^7 cpm/μg of C1s (0.15–0.30 mol of label/mol of C1s). The concentration of C1s was determined by using the value of $E_{280,1\%} = 13.7$ (Busby & Ingham, 1988). Further tests to check that the labeling procedure did not affect dimerization were performed by sedimentation equilibrium of mixtures of labeled and cold C1s (see Results section for details).

Ca^{2+} Equilibration of C1s. To avoid metal contamination, plasticware and dialysis tubing were treated before use according to Potter et al. (1983). Th C1s was dialyzed against Hepes buffer with 1 mM EGTA and then extensively dialyzed against metal-free Hepes buffer. The contaminating Ca^{2+} of the latter (0.10 ± 0.01 μM) was measured using the fluorescent Ca^{2+} indicator fluo-3 AM and a calcium calibration kit, both from Molecular Probes Inc. (Minta et al., 1989; Tsien & Pozzan, 1989). Samples of C1s at a given protein concentration were then equilibrated with the required Ca^{2+} concentration by dialysis against Hepes/Ca^{2+} buffer (500 × volume, 3 changes, 10 °C), prepared by taking into account the Ca^{2+} contaminant in the buffer and then adding Ca^{2+} as necessary from a 0.5 M $CaCl_2$ stock solution [prepared according to Forstner and Manner (1971)]. After equilibrium dialysis the free Ca^{2+} was checked by a Ca^{2+} electrode (Whatman) in the 5 mM–10 μM region and using fluo-3 in the 1–0.1 μM region. In the low calcium experiments (nanomolar concentration) a Ca^{2+}/EGTA buffer was used (Tsien & Pozzan, 1989).

Measurement of Sedimentation Equilibrium. Experiments were performed using the methodology of Attri & Minton (1983) with modifications. Small quartz tubes [made by shortening quartz NMR tubes, Wilmad Glass Co., as described in Attri and Minton (1983)] containing 40 μL of protein sample (4-mm column height) above 50 μL of immiscible fluorocarbon FC-47 (3M) were centrifuged at 6500–7000 rpm in SW-41 or TLS-55 swinging bucket rrotors for at least 24 h at 10 °C to assure attainment of sedimentation equilibrium. A total concentration of 2.5 mg/mL of dextran-70 (Polysciences Inc.) was added to dilute protein samples (less than 0.2 mg/mL) to stabilize the equilibrium gradients during subsequent handling (Minton, 1989; Pollet, 1985). Depending upon total protein concentration, following the conclusion of centrifugation, each tube was scanned in a Perkin-Elmer 320 spectrophotometer equipped with a scanning accessory to yield a profile of absorbance at 280 nm vs radial position (Attri & Minton, 1983) and/or fractionated with a Brandel automated microfractionator onto Beckman ready caps. Fractions were then counted on a Beckman LS 3801 scintillation counter to obtain a profile of cpm vs radial distance (Attri & Minton, 1986; Darawshe et al., 1992). Samples containing protein concentrations greater than 4 μM were scanned, those below 4 μM were fractionated, and those at 4 μM were both scanned and fractionated to check consistency of the two experimental methods. Precision of the measurements in the UV scanner and microfractionator was determined experimentally, and

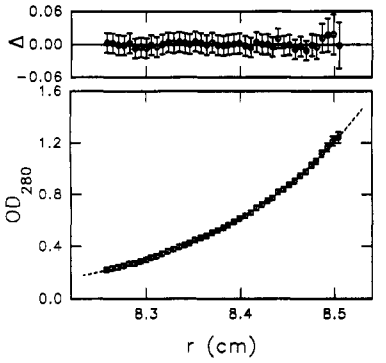

FIGURE 1: Equilibrium centrifugation of human complement C1s plotted as absorbance vs radial distance. Lower panel: symbols represent data obtained for c_{tot} = 15 μM, [Ca^{2+}] = 1 μM, error bars represent ±2 SEM, and the dashed line represents the best fit of eq 12 to obtain the weight-average molecular weight. Upper panel: best-fit residuals vs radial distance.

the results obtained are well represented by the following relations:

$$\sigma(\text{OD,280 nm}) = \begin{cases} 8.93 \times 10^{-3} & (\text{OD} \leq 1.0) \\ 8.93 \times 10^{-3} \exp[3.20\,(\text{OD} - 1.0)] & (\text{OD} > 1.0) \end{cases} \quad (11a)$$

$$\sigma(\text{cpm}) = 190 + 0.032(\text{cpm}) - 5.75 \times 10^{-8}(\text{cpm})^2 \quad (11b)$$

where σ(OD,280 nm) and σ(cpm) are the absolute values of standard deviation for absorbance at 280 nm and radioactivity measurements, respectively.

Data Analysis. The concentration of an ideally sedimenting mixture of species is given as a function of radial position by

$$c_{tot}(r) = c_{tot}(r_f) \exp\{M_w(1 - \bar{v}\rho)\omega^2(r^2 - r_f^2)/2RT\} \quad (12)$$

where c_{tot} is the total concentration of solute, $\bar{v}$ is the partial specific volume of solute (assumed to be the same for all species), ρ is the solvent density, ω is the angular velocity, and r_f is a reference radial position. The partial specific volume of C1s at 10 °C (0.706 mL/g) was calculated from the amino acid and sugar composition (Mackinnon et al., 1987; Tosi et al., 1987; Sim et al., 1977), according to Durchschlag (1986). Since the concentration of solute did not vary by more that a factor of 5 at most from meniscus to base in any given equilibrium run, it was assumed that the weight-average molecular weight of solute would vary only slightly throughout the cell and that eq 12 with a constant value of M_w would describe the experimentally observed solute gradient. Equation 12 was fitted to each gradient by nonlinear minimization of χ^2, using the modified Nelder–Mead downhill simplex algorithm (Press et al., 1986, Hsu & Minton, 1991). Equation 12 was found to fit all experimental gradients to well within experimental precision. In Figure 1 an experimental gradient is plotted together with the best-fit calculated gradient for a "worst case" situation, in which approximately half of the solute is present as monomer and half as dimer. Confidence limits (95%) for M_w were determined by constrained best-fits as described in Hsu and Minton (1991). In this fashion a table of M_w as a function of c_{tot} and [Ca^{2+}] was constructed, which was subsequently analyzed in the context of models for ligand-linked self-association as described below.

Models for ligand-linked association equilibria described in the theoretical section were fitted to the data as follows. A global χ^2 function [compare eq 19 of Hsu and Minton (1991)] was defined for the variables n_{11}, n_{12}, log K_{11}, log K_{12}, n_{21}, n_{22}, log K_{21}, log K_{22}, and log K_0. The global χ^2 function depends upon the measured and calculated values of M_w at

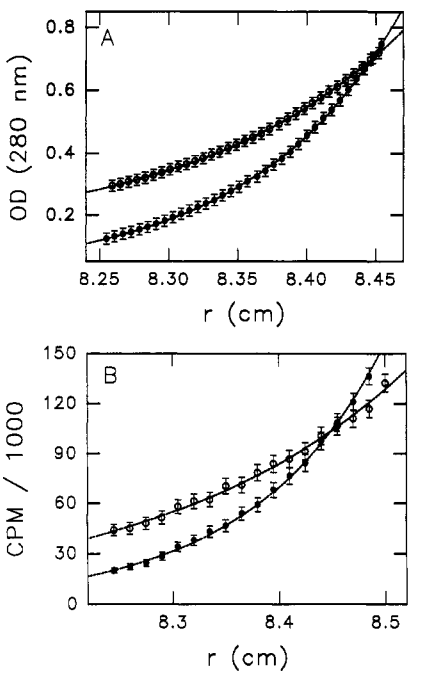

FIGURE 2: Effect of Ca^{2+} on equilibrium centrifugation of C1s at two different protein concentrations. Panel A: equilibrium gradients of absorbance vs radial distance (c_{tot} = 1.6 × 10^{-5} M); filled points, [Ca^{2+}] = 5 mM; open points, [Ca^{2+}] = 1 nM. Curves represent best fits to eq 12. Panel B: equilibrium gradients of radioactivity vs radial distance (c_{tot} = 1.25 × 10^{-7} M). Symbols and curves as in panel A.

each value of c_{tot} and [Ca^{2+}]. The number and distribution of binding sites was fixed by constraining the values of n_{11}, n_{12}, and n_{21}, and n_{22}. Then the χ^2 function was minimized using the modified simplex algorithm (Press et al., 1986) to obtain best-fit values of log K_0 and log K_{ij} for each class of sites with $n_{ij} > 0$.

RESULTS

To exclude the possibility that radioiodination affects the association properties of C1s, we centrifuged mixtures of labeled and unlabeled C1s (1.7 mg/mL total protein) to equilibrium in the presence of low (1 nM) and high (5 mM) concentrations of Ca^{2+}. After reaching equilibrium each sample was first scanned optically and then fractionated and counted. The adsorbance and radioactivity gradients were fitted to eq 12. The results obtained for the absorbance gradients are presented in Figure 2A. The best-fit values of M_w for the low and high Ca^{2+} concentrations are 8.0 × 10^4 and 1.62 × 10^5, respectively, corresponding well to literature values for monomeric and dimeric C1s (Tschopp et al., 1980). Weight-average molecular weights obtained by fitting the radioactivity gradients obtained from the same sample (not shown) were identical to those obtained by absorbance within experimental uncertainty (±2.5 × 10^3), both at low Ca^{2+} concentration (no association) and at high Ca^{2+} concentration (essentially complete dimerization). Thus, the label does not affect association, confirming the work of Illy et al. (1991).

With labeled C1s it was possible to extend measurements to very low concentration. Equilibrium radioactivity gradients of labeled C1s at 1.25 × 10^{-7} M at the same two high and low Ca^{2+} concentrations are plotted in Figure 2B together with the calculated best fit of eq 12 to each data set. The best-fit values of M_w for the low and high Ca^{2+} concentrations are 7.9 × 10^4 and 1.43 × 10^5, respectively. The latter value indicates that, at this very low protein concentration, C1s is incompletely dimerized even in the presence of high Ca^{2+}.

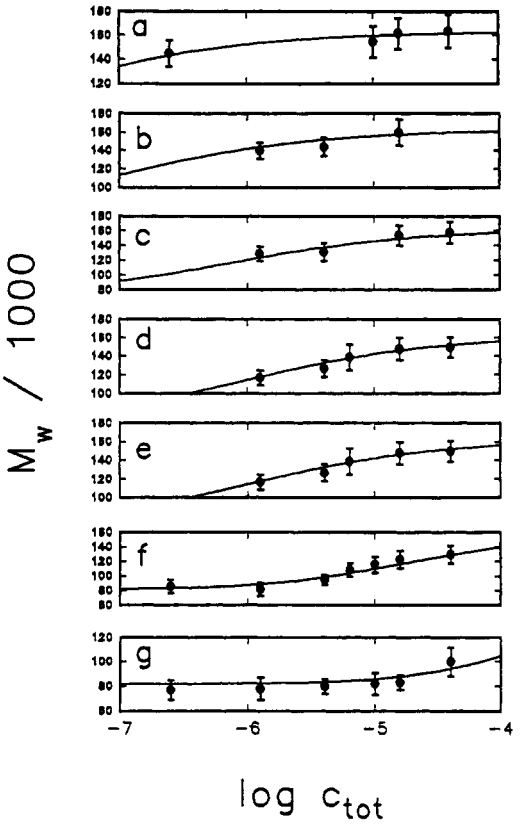

FIGURE 3: Weight-average molecular weight of C1s plotted as a function of log c_{tot} for different values of log [Ca^{2+}]. Each data point represents the mean of best-fit values of M_w obtained from 3–6 replicate experiments, and the error bars represent ±2 SEM. The plotted curves were calculated as described in the Theory section, for model 8 (Table I), with the best-fit parameter values given in the legend to Table I. The free Ca^{2+} concentrations (molar) are as follows: a, 5.0×10^{-3}; b, 1.0×10^{-3}; c, 1.0×10^{-4}; d, 1.0×10^{-5}; e, 1.0×10^{-6}; f, 1.0×10^{-7}; g, 1.0×10^{-9}.

Experimentally measured values of M_w obtained in this manner over a range of concentrations of total protein and free Ca^{2+} are presented in Figure 3. The data indicate that, at high protein concentration, some dimer forms even at very low Ca^{2+} levels, and again that, at low protein concentration, some monomer exists even at physiological levels of Ca^{2+}. It is also clear that the state of association is influenced by very low levels of Ca^{2+}, in the submicromolar range. Various models were fitted to the combined data as described above. The probability that the best-fit value of χ^2 for each model is less than that obtained from a random distribution of χ^2 was calculated (Press et al., 1986; Hsu & Minton, 1991). A model was considered to be consistent with the data (i.e., not excluded by the data) only if this probability exceeds 0.05. The results of this analysis are summarized in Table I.

It is evident from eq 9 that Ca^{2+} will induce self-association only if the total amount of Ca^{2+} bound by 1 mol of dimer exceeds that bound by 2 mol of monomer. This requires that there be an increase in the number of binding sites and/or the affinity upon dimerization. Although all of the models listed in Table I have the potential to meet these criteria, only three of them (8, 13, and 14) satisfied the χ^2 test described above. Model 8 can be viewed as a limiting case of model 13 in which one of the two classes of sites on the monomer has such a low affinity for Ca^{2+} that none is bound over the range of Ca^{2+} concentrations employed in the present study. In fact, the best fit of model 13 to the sedimentation data yields this limiting case, i.e., $\log K_{12} < 2$ with all other best-fit parameter values similar to those obtained with model 8. Model 14, while marginally consistent with the sedimentation data, can be rejected as grossly incompatible with reported Ca^{2+} binding data (see below). Thus, the simplest model consistent with the data is model 8. The parameters obtained by the fitting procedure with model 8 were used to generate the calculated gradient and residuals plotted in Figure 3 as well as the surface in Figure 4, where the data are reproduced in three-dimensional stereoview. According to this model, the monomer contains a single Ca^{2+} binding site with $K \simeq 3 \times 10^5$ M^{-1}, and the dimer contains three independent Ca binding sites, two having a Ca^{2+} affinity lower than that of the monomer ($K \simeq 3 \times 10^4$ M^{-1}) and a third of much higher affinity ($K \simeq 1 \times 10^8$ M^{-1}) that provides the driving force for dimerization.

Table I: Models for Which Global Fitting Was Attempted to Entire Set of Data, in Order of Increasing Complexity[a]

	monomer		dimer			
model	first class, n_{11}	second class, n_{12}	first class, n_{21}	second class, n_{22}	best fit χ^2	P (best fit χ^2)
1	0	0	1	0	168	0.00
2	0	0	2	0	319	0.00
3	0	0	3	0	364	0.00
4	1	0	1	0	153	0.00
5	1	0	2	0	158	0.00
6	1	0	3	0	156	0.00
7	1	0	1	1	154	0.00
8	1	0	2	1	63	0.89
9	1	0	2	2	139	0.00
10	1	1	2	0	159	0.00
11	1	1	3	0	188	0.00
12	1	1	4	0	178	0.00
13	1	1	2	1	68	0.77
14	1	1	2	2	96	0.07

[a] Data from Figure 3; $n = 82$. The precision of the data permit all except models 8, 13, and 14 to be ruled out with 95% confidence. Model 8, which is the simplest of the three acceptable models, also yields the best global fit. The best-fit values of the parameters of model 8, with 95% confidence limits, are $\log K_0 = 3.3$ (+0.7), $\log K_{11} = 5.4$ (+0.15, −0.10), $\log K_{21} = 4.4$ (+1.1, −0.9), and $\log K_{22} = 8.0$ (−0.8) (see eq 8).

Using model 8 together with the best-fit parameter values obtained as described above, a number of derivative quantities were calculated to illustrate the effect of Ca^{2+} on self-association. The dependence of log K upon log [Ca^{2+}], calculated using eq 8, is plotted in Figure 5. It is clear that the dimerization constant becomes sensitive to Ca^{2+} beginning near 10^{-8} M. The lack of sensitivity of the dimerization constant to changes in Ca^{2+} concentration in the vicinity of 10^{-5} M reflects equal binding of Ca^{2+} to the monomer and dimer in this region. The weight fraction of dimer and the average number of moles of Ca^{2+} ions bound per mole of C1s are plotted as a function of log [Ca^{2+}] for several total protein concentrations in Figure 6, panels A and B, respectively.

DISCUSSION

In order to discriminate between alternate schemes of reversible association and determine the values of equilibrium constants to within reasonable limits of uncertainty, it is necessary to obtain data over as broad a range of concentrations of the interacting components as possible (Hsu & Minton, 1991). This principle is well illustrated by the results of the present study (Figures 3 and 4). Our data, spanning over 6 orders of magnitude in calcium concentration and over 2 orders of magnitude in protein concentration, enabled us to rule out several simple models for linkage of calcium binding and self-association of C1s as inadequate. According to the simplest model capable of accommodating the entire data set, both monomeric and dimeric C1s bind Ca^{2+} to a single site per monomer. The dimer contains an additional high-affinity Ca^{2+} binding site, which presumably lies at the interface

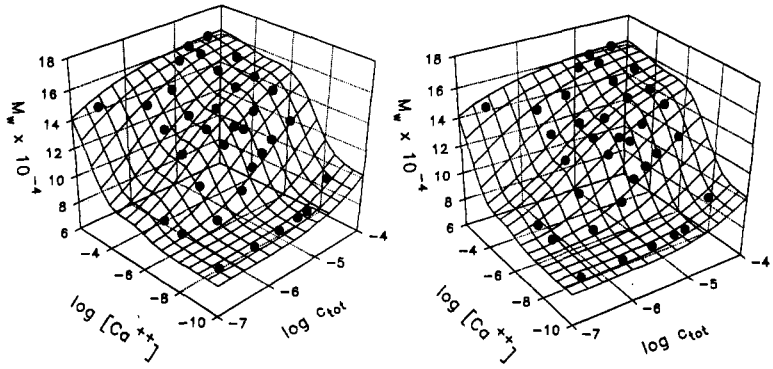

FIGURE 4: Stereo plot of M_w as a function of log [Ca^{2+}] and log c_{tot}. Data points are as described in caption to Figure 3. Surface is calculated using model 8 (Table I), with the best-fit parameter values given in the legend to Table I.

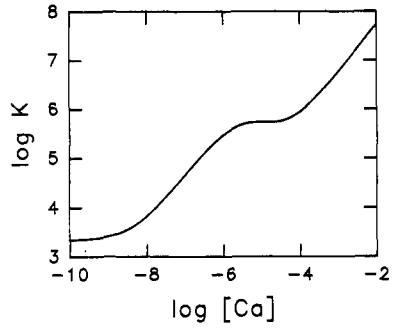

FIGURE 5: Dependence of the C1s dimerization constant on Ca^{2+} concentration. Log K was calculated as a function of log [Ca^{2+}] from eq 8 using the parameters of model 8 as described in text.

between the two monomeric subunits in the dimer, as proposed by Illy et al. (1991).

Thielens et al. (1990b) concluded from a Scatchard analysis of Ca^{2+} binding data obtained via equilibrium dialysis that C1s, as well as its N-terminal α fragment, contains three identical Ca^{2+} binding sites per mole of dimer with an affinity corresponding to log $K_c = 4.7$ for C1s and 4.4 for the fragment. Their data, as well as the earlier data of Villiers et al. (1980), corrected according to Thielens et al. (1990b), are plotted in Figure 7. The calculated isotherm for the single site class model with their parameter values is represented by the dashed line. The solid line in Figure 7 is the Ca^{2+} binding isotherm calculated from the present model. The binding data do not seem to provide any indication of the high-affinity Ca^{2+} binding site detected in the present study. This may be due to the different conditions under which the earlier studies were carried out: 4 °C vs 10 °C in the present study, and triethanolamine buffer vs Hepes buffer in the present study. Also, we have no information regarding the precision of the binding data; we note that the two experimental data sets diverge from each other by as much as the divergence between the data and our calculated isotherm. Finally, our studies were carried out over a range of free calcium concentrations extending as low as 10^{-9} M, while the binding studies were limited to free Ca^{2+} concentrations in excess of 5×10^{-6} M. The sedimentation equilibrium approach used here provides an indirect but sensitive method for detecting Ca^{2+} binding at low concentration by measuring its effect on the state of association. For this reason we believe that our study was considerably more sensitive to the presence of high-affinity Ca^{2+} binding sites. A careful comparison of the data in panels f and g of Figure 3 reveals an unambiguous change in the state of association of C1s on increasing [Ca^{2+}] from 10^{-9} to 1×10^{-7} M. Although the resulting model disagrees quantitatively with the earlier single-class-of-sites model of Ca^{2+} binding to C1s, it does confirm the finding of Thielens et al. (1990b) of three binding sites in the limit of high calcium concentration.

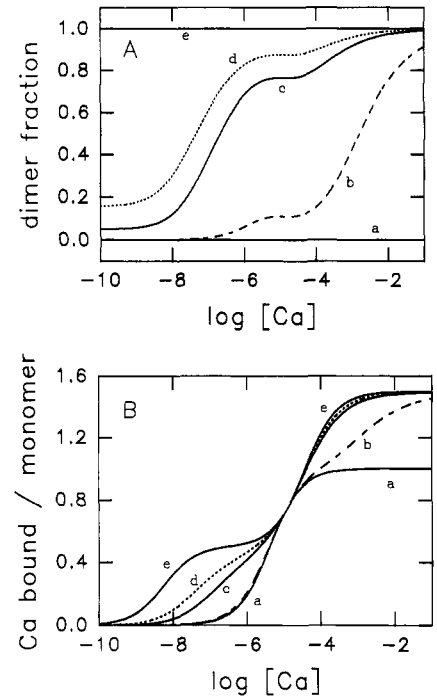

FIGURE 6: Dependence of Ca^{2+} binding and self-association of C1s on free Ca^{2+} concentration. Panel A: Weight fraction of dimer calculated as a function of log [Ca^{2+}] as described in text for the following total protein concentrations: (a) limiting low concentration, (b) 1.25×10^{-7} M, (c) 1.25×10^{-5} M, (d) 5×10^{-5} M, and (e) limiting high concentration. Panel B: total Ca^{2+} bound $[(n_{1b} + n_{2b})/2]$ expressed per mol of C1s, plotted as a function of log [Ca^{2+}], as described in text, for the same total protein concentrations as in panel A.

Dahlback et al. (1990) described a novel type of very high affinity calcium-binding site (K on the order of 10^9 M^{-1}) in the β-OH-Asp-containing epidermal growth factor (EGF)-like domains of vitamin K-dependent protein S. C1r and C1s also have EGF-like domains that are β-hydroxylated at homologous Asn residues, fully in C1r but only partially in C1s. Since dimerization of C1s seems quantitative in spite of only partial hydroxylation, it seems that this posttranslational modification is not important for Ca^{2+}-dependent self-association. The work of Thielens et al. (1990) clearly demonstrates that additional domains beyond the EGF-like domains are required for Ca^{2+} binding and self-association.

The evidence presented here for a high-affinity Ca^{2+} binding site in C1s dimers helps explain an earlier observation regarding the effect of Ca^{2+} on the low-temperature thermal transition in C1s, a transition that involves the EGF-containing α region (Medved et al., 1989). In that study it was shown that mere absence of EDTA was sufficient to elevate the low-temperature T_m by several degrees. Perhaps residual Ca^{2+} in the untreated

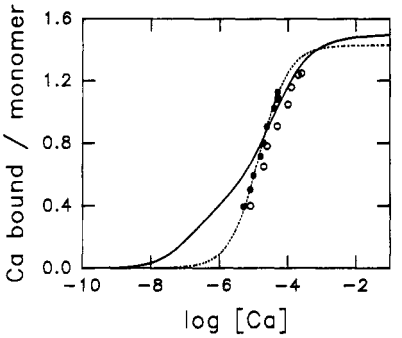

FIGURE 7: Number of Ca^{2+} ions bound per mol of C1s plotted as a function of log [Ca^{2+}]. Open symbols: data of Villiers et al. (1980) (see text). Filled symbols: data of Thielens et al. (1990b). Dotted line: isotherm calculated from parameter values given by Thielens et al. (1990b). Solid line: isotherm calculated from present model as described in text for $c_{tot} = 10^{-5}$ M.

buffers was sufficient to cause significant dimerization at the relatively high C1s concentrations used in the calorimetric measurements.

A careful study of the calculated curves in Figure 6 can provide some insight into the equilibrium average state of association of C1s under various conditions of interest. At one extreme, in the limit of high [C1s] where dimerization is already complete, curves e show that Ca^{2+} would bind first to the high-affinity site on the dimer and later to the two low-affinity sites that are also present on the monomer but whose affinities are decreased slightly in the dimer. Curves a show that, at the opposite extreme, in the limit of low [C1s], no dimerization occurs, the high-affinity site is never formed, and binding would be limited to the monomer, reaching saturation at only 1 mol/mol as opposed to 1.5 in the other cases. At laboratory concentrations (10–50 μM), C1s will exist as a mixture of monomer and dimer depending on the Ca^{2+} concentration (curves c and d). At the concentrations found in blood (~0.4 μM; Cooper, 1985), C1s, in the absence of C1r, would be incompletely dimerized and sensitive to changes in the millimolar concentrations of total Ca^{2+} which prevail there (curves b, 0.125 μM C1s). Of course, under normal conditions, C1s in blood is accompanied by equimolar concentrations of C1r, which disrupts the normal mode of association of C1s and forms a heterotetramer that circulates in association with C1q (Cooper, 1985). An extension of the present study to encompass calcium-linked interactions between C1s and C1r is underway. The results presented here will be essential to an understanding of the more complex heteroassociation and the mechanism by which the α domains of C1s change their allegiance from one of self-association toward one of heteroassociation with the homologous α regions of C1r.

ACKNOWLEDGMENT

We thank Dr. T. F. Busby, American Red CRoss, for the preparation of human C1s. Thanks also to Drs. Peter Jeffrey and Dan Sackett for helpful comments about the manuscript.

REFERENCES

Arlaud, G. J., Chesne, S., Villiers, C. L., & Colomb, M. G. (1980) *Biochim. Biophys. Acta 616*, 105–115.

Arlaud, G. J., Gagnon, J., Villiers, C. L., & Colomb, M. G. (1986) *Biochemistry 25*, 5177–5182.

Arlaud, G. J., Colomb, M. G., & Gagnon, J. (1987a) *Immunol. Today 8*, 106–111.

Arlaud, G. J., Van Dorsselaer, A., Bell, A., Mancini, M., Aude, C., & Gagnon, J. (1987b) *FEBS Lett 222*, 129–134.

Attri, A. K., & Minton, A. P. (1983) *Anal. Biochem. 133*, 142–152.

Attri, A. K., & Minton, A. P. (1986) *Anal. Biochem. 152*, 319–328.

Attri, A. K., & Minton, A. P. (1987) *Anal. Biochem. 162*, 409–419.

Busby, T. F., & Ingham, K. C. (1988) *Biochemistry 27*, 6127–6135.

Cooper, N. R. (1985) *Adv. Immunol. 37*, 151–216.

Dahlback, B., Hildebrand, B., & Linse, S. (1990) *J. Biol. Chem. 265*, 18481–1849.

Darawshe, S., Rivas, G., & Minton, A. P. (1992) *Anal. Biochem.* (submitted for publication).

Durchschlag, H. (1986) in *Thermodynamic Data for Biochemistry and Biotechnology* (Hinz, H. J. Ed.), pp 45–128, Springer-Verlag, Berlin.

Forstner, J., & Maner, J. F. (1971) *Biochem. J. 124*, 563–571.

Harding, S. E., & Rowe, A. J., Eds. (1992) *Analytical Ultracentrifugation in Biochemistry and Polymer Science*, Royal Society of Chemistry, Cambridge, England (in press).

Howlett, G. J. (1987) *Methods Enzymol. 150*, 447–463.

Hsu, C. S., & Minton, A. P. (1991) *J. Mol. Recog. 4*, 93–104.

Illy, C., Thielens, N. M., Gagnon, J., & Arlaud, G. J. (1991) *Biochemistry 30*, 7135–7141.

Johnson, M. L., & Frasier, S. G. (1985) *Methods Enzymol. 117*, 301–342.

Mackinnon, C. M., Carter, P. E., Smyth, S. J., Dunbar, B., & Fothergill, J. E. (1987) *Eur. J. Biochem. 169*, 547–553.

Medved, L. V., Busby, T. F., & Ingham, K. C. (1989) *Biochemistry 28*, 5408–5414.

Minta, A., Kao, J. P. Y., & Tsien, R. Y. (1989) *J. Biol. Chem. 264*, 8171–8178.

Minton, A. P. (1975) *J. Mol. Biol. 95*, 289–307.

Minton, A. P. (1989) *Anal. Biochem. 176*, 209–216.

Minton, A. P. (1990) *Anal. Biochem. 190*, 1–6.

Muramatsu, N., & Minton, A. P. (1989) *J. Mol. Recog. 1*, 166–171.

Pollet, R. J. (1985) *Methods Enzymol. 117*, 3–27.

Potter, J. D., Strang-Brown, P., Walker, P. L., & Iida, S. (1983) *Methods Enzymol. 102*, 135–143.

Press, W. H., Flannery, B. P., Teukolsky, S. A., & Vetterling, W. T. (1986) *Numerical recipes. The art of scientific computing*, Cambridge University Press, Cambridge, England.

Record, M. T., Jr., Anderson, C. F., & Lohman, T. M. (1978) *Q. Rev. Biophys. 11*, 103–178.

Saroff, H. A. (1991) *Biochemistry 30*, 10085–10090.

Scatchard, G. (1949) *Ann. N.Y. Acad. Sci. 51*, 660–672.

Schumaker, V. N., Zavodszky, P., & Poon, P. H. (1987) *Annu. Rev. Immunol. 5*, 21–42.

Sim, R. B., Porter, R. R., Reid, K. B., & Gigli, I. (1977) *Biochem. J. 163*, 219–227.

Thielens, N. M., Van Dorsselaer, A., Gagnon, J., & Arlaud, G. J. (1990a) *Biochemistry 29*, 3570–3578.

Thielens, N. M., Aude, C. A., Lacroix, M. B., Gagnon, J., & Arlaud, G. J. (1990b) *J. Biol. Chem. 265*, 14469–14475.

Tosi, M., Duponchel, C., Meo, T., & Julier, C. (1987) *Biochemistry 26*, 8516–8524.

Tschopp, J., Villiger, W., Fuchs, H., Kilchher, E., & Engel, J. (1980) *Proc. Natl. Acad. Sci. U.S.A. 77*, 7014–7018.

Tsien, R., & Pozzan, T. (1989) *Methods Enzymol. 172*, 230–262.

Valet, G., & Cooper, N. R. (1974) *J. Immunol. 112*, 339–350.

Villiers, C. L., Arlaud, G. J., Painter, R. H., & Colomb, M. G. (1980) *FEBS Lett. 117*, 289–294.

Wyman, J., & Gill, S. J. (1990) *Binding and linkage: functional chemistry of biological macromolecules*, University Science Books, Mill Valley, CA.

Registry No. Activated C1s, 80295-70-1; Ca, 7440-70-2.